communications biology

Article

https://doi.org/10.1038/s42003-024-06741-1

The role of halophyte-induced saline fertile islands in soil microbial biogeochemical cycling across arid ecosystems

Check for updates

Shuai Zhao[1], Marcel G. A. van der Heijden[2], Samiran Banerjee[3], Jun-jie Liu[4] ✉, Hai-dong Gu[4], Na Zhou[1], Chuan-hua Yin[5] ✉, Bin Peng[1], Xu Liu[6], Bao-zhan Wang[6] & Chang-yan Tian[1]

Halophyte shrubs, prevalent in arid regions globally, create saline fertile islands under their canopy. This study investigates the soil microbial communities and their energy utilization strategies associated with tamarisk shrubs in arid ecosystems. Shotgun sequencing revealed that high salinity in tamarisk islands reduces functional gene alpha-diversity and relative abundance compared to bare soils. However, organic matter accumulation within islands fosters key halophilic archaea taxa such as *Halalkalicoccus*, *Halogeometricum*, and *Natronorubrum*, linked to processes like organic carbon oxidation, nitrous oxide reduction, and sulfur oxidation, potentially strengthening the coupling of nutrient cycles. In contrast, bare soils harbor salt-tolerant microbes with genes for autotrophic energy acquisition, including carbon fixation, H_2 or CH_4 consumption, and anammox. Additionally, isotope analysis shows higher microbial carbon use efficiency, N mineralization, and denitrification activity in tamarisk islands. Our findings demonstrate that halophyte shrubs serve as hotspots for halophilic microbes, enhancing microbial nutrient transformation in saline soils.

In arid ecosystems, soil microbiomes play a pivotal role in steering soil nutrient biogeochemical cycling[1]. However, microbial life contends with mutable challenges, including nutrient limitations, aridity, and salinity[2]. The presence of scattered plants in arid ecosystems prompts the redistribution of soil resources from bare soil interspaces to beneath shrub canopies, resulting in the formation 'fertile islands' which provide a refugium for microbiomes. These islands host diverse microbiomes that significantly contribute to soil nutrient cycling in hyper-arid environments[3–5].

Halophytes, renowned for their salt and drought tolerance, are widespread in global arid regions. Taking tamarisk (commonly known as salt cedar) as an illustration, the majority of *Tamarix* species originate in Eurasia, with at least five species proving invasive and densely distributed in drylands spanning the Midwest of the USA, Northern and Southern Africa, Central Asia, and Northern China (Global Biodiversity Information Facility, http://www.gbif.org)[6]. The exudates and leaf litter of these plants elevate soil salinity under the plant canopy[7,8], giving rise to what are termed 'saline fertile islands' in arid landscapes[9]. It is crucial to recognize that salinity is a key factor shaping microbial communities and can impede various microbial activities[10–12]. In the case of halophytes, their presence generates unique niches for microbial communities, which, in turn, exert complex and uncertain effects on microbially mediated nutrient cycling within arid ecosystems. Therefore, understanding the microbial characteristics below ground associated with halophytes is indispensable for formulating strategies to manage crucial soil functions and preserve the services provided by these fragile environmental systems.

Microorganisms represent the biochemical engines of global element cycles[13,14]. Within this complex interplay, functional genes encoding enzymes specific to redox reactions hold the potential to unveil underlying biogeochemical processes and the microbial agents orchestrating them[15]. For instance, researchers have utilized bipartite function-taxon networks derived from metagenomic contigs to identify microbes that act as lynchpins in linking nutrient cycles within forest soils in eastern China,

[1]State Key Laboratory of Desert and Oasis Ecology, Xinjiang Institute of Ecology and Geography, Chinese Academy of Sciences, Urumqi, 830011, China. [2]Department of Plant and Microbial Biology, University of Zurich, Zurich, 8008, Switzerland. [3]Department of Microbiological Sciences, North Dakota State University, Fargo, ND, 58102, USA. [4]State Key Laboratory of Black Soils Conservation and Utilization, Northeast Institute of Geography and Agroecology, Chinese Academy of Sciences, Harbin, 150081, China. [5]School of Tea and Food Science, Wuyi University, Wuyishan, 354300, China. [6]Department of Microbiology, College of Life Sciences, Nanjing Agricultural University, Nanjing, 210000, China. ✉e-mail: liujunjie@iga.ac.cn; yinchh2006@126.com

emphasizing the sensitivity of functional gene composition and diversity to soil pH[16]. In a recent metagenomic investigation, it was revealed that shrub-induced 'fertile islands' in desert ecosystems provoke shifts in soil microbial energy use strategies, favoring the proliferation of copiotrophic microbes and microbes that cannot use atmospheric trace gases to support their activity, compared to bare soils[5]. However, metagenomic studies examining microbial patterns in arid ecosystems, especially those focusing on the community's biogeochemistry in saline soils, are still limited. Specific questions persist regarding whether the drivers of microbial diversity and the sensitivity of functional gene composition in halophyte-induced islands differ from their surrounding bare saline soils. Additionally, it remains unclear whether the concentration of salt in the islands reduces diversity of microbial functional genes, and if microbial taxa and genes are selectively enriched in these islands, playing a pivotal role in driving specific biogeochemical cycles.

This study employs tamarisk islands as a model to unveil soil microbial functional profiles and their ability to process biogeochemical reactions within and beyond halophyte islands. Our dataset encompassed soils from three distinct arid ecosystems near the Taklimakan Desert, China. Using cultivation-independent metagenomic sequencing, we linked biomarker genes for soil biogeochemical cycles with their respective microbial taxa. Additionally, stable isotope tracing enabled us to delineate distinct microbial carbon and nitrogen processing intensities in soils beneath shrub canopies and in bare soils. We hypothesized that the heterogeneity of soil properties induced by halophyte favors specific microbial taxa and enhances microbial metabolic efficiency, subsequently fortifying soil biogeochemical processes. This exploration can offer valuable insights into the intricate relationship between halophyte islands and microbial-driven biogeochemical cycles in arid ecosystems.

Results

Linking soil chemistry to functional gene composition and diversity

We observed the soil variables, including salinity, SOM (soil organic matter), TN (total nitrogen), and NH_4^+-N, were significantly higher in soils under shrubland (inner) compared to bare areas (outer) across three arid ecosystems (Fig. 1B; Fig. S1). KEGG annotation results revealed that, except for the bare soil in tamarisk shrubland, other soils did not show significant variation in the proportion of unannotated genes, which ranged from 44% to 47% across samples (Fig. S2). Metagenomic profiling indicated that the most abundant community members were archaea from the *Euryarchaeota* phylum, ranging from 48.2% to 89.5% (Fig. S3). In the inner soils, *Halobacteria* were particularly dominant, comprising 76.8% to 89.2%. In the outer soils, *Halobacteria* (46.5% to 59.1%), *Gemmatimonadetes* (6.6% to 8.9%), and *Actinobacteria* (2.9% to 4.0%) were found in abundance (Fig. S3).

Salinity was identified as the primary driver of soil community, and it showed a negative correlation with functional gene richness index ($r = -0.54$, $P < 0.001$) and Shannon index ($r = -0.36$, $P < 0.001$) (Fig. 1C; Fig. S4). The functional gene composition was roughly divided into two groups (Supplementary Data 1), inner and outer, along the salinity gradient based on PCoA analysis (Fig. 1D; Fig. S5). The variation of soil metagenomes in the outer group was mainly determined by salinity and AK (available potassium), whereas in the inner group, it was mainly determined by NO_3^--N and SOM (Fig. 1E; Fig. S6).

Microbial genes related to soil C, N, and S biogeochemical cycles

There were significant changes in the abundance of genes associated with carbon (C), nitrogen (N), and sulfur (S) cycles in arid ecosystems (Supplementary Data 2). Specifically, we found that soils beneath tamarisk canopies contained a significant higher abundance of genes involved in carbohydrate metabolism. Microbial genes associated with pectin metabolism increased in inner soils from MS to SD. For example, the relative abundance of genes responsible for the conversion of rhamnogalacturonan to RG-oligosaccharides exhibited a 2.2-fold increase. In contrast, genes related to hemicellulose metabolism decreased in inner soils. Specifically, the relative abundance of genes responsible for the conversion of xyloglucan to xylo-gluco-oligosaccharide decreased by 76.5% (Fig. S7). Among the carbon-cycling biomarker genes, organic carbon oxidation (C-S-01) and anaerobic fermentation (C-S-06) were the dominant processes, comprising 79% and 6% of all contigs, respectively (Fig. 2; Supplementary Data 3). Notably, organic carbon oxidation and fermentation were more prominent in inner soils compared to outer soils, and showed a negative correlation with soil salinity. The genes for aerobic respiration processes, including methanotrophy, H_2 oxidation, and acetate oxidation, all had their highest abundance in the outer soils. *Euryarchaeota* were the main contributors to both organic carbon oxidation and anaerobic fermentation, as revealed by identifiable taxa (Fig. S8; Supplementary Data 4).

In terms of nitrogen cycling, the dominant biomarker genes were associated with nitrite reduction (N-S-05) and nitric oxide reduction (N-S-06), and their abundance was higher in inner soils compared to outer soils (Fig. 3). Nitrite oxidation (N-S-03), nitrite reduction (N-S-05), and nitrous oxide reduction (N-S-07) showed a positive correlation with soil salinity, and *Euryarchaeota* were the most frequently assigned taxa and played a dominant role in these pathways (Fig. S8). Interestingly, the gene abundance for anammox (anaerobic ammonium oxidation) (N-S-09), which is associated with autotrophic nutrition, was over twice as high as that in the outer soils (Fig. 3; Supplementary Data 5).

Sulfur cycling biomarker genes were dominated by sulfur oxidation (S-S-03) and sulfite oxidation (S-S-04)/sulfate reduction (S-S-05), comprising 1.7% and 1.5% of all contigs, respectively (Fig. 4). Compared to inner soils, outer soils had a higher gene abundance in sulfur oxidation (S-S-03) and sulfite oxidation (S-S-04)/sulfate reduction, and showed an increasing trend, negatively correlated with salinity. *Euryarchaeota* played a dominant role in sulfur oxidation (S-S-03), whereas *Cyanobacteria* contributed to substrate sulfite oxidation (S-S-04) (Fig. S8; Supplementary Data 6).

Linking biogeochemical processes to microbial taxa using a function-taxa bipartite network

The results demonstrate that nutrient cycling in the outer soils is primarily driven by taxa such as *Gemmatimonas* and halophilic archaea, which including *Haloarcula*, *Halococcus*, *Haloferax*, *Halosimplex*, and *Haloterrigena* (Fig. S9). In contrast, inner soils harbor a more diverse community of halophilic archaea taxa, including *Halobacterium*, *Halalkalicoccus*, *Halomicrobium*, *Halogeometricum*, *Halorubrum*, among others. Function-taxa bipartite network analysis revealed the formation of six clusters in outer soils, each consisting of genes associated with biogeochemical processes and their corresponding taxa (Fig. 5). In inner soils, four clusters were observed. Within each cluster, both biogeochemical processes and coupling processes appeared to be potentially driven by taxa requiring similar redox states.

In outer soils, two clusters were associated with the potential coupled carbon-nitrogen (C-N) cycle (Fig. 5). The first cluster was dominated by *Euryarchaeota*, such as *Halomicrobium*, *Halapricum*, and unclassified *Halobacteriales*, and contained genes involved in five pathways. The second cluster was dominated by *Salinarchaeum* and *Rhodothermus* and contained genes involved in two pathways, i.e., methanotrophy (C-S-08) and nitrous oxide reduction (N-S-07). Additionally, two clusters related to carbon and sulfur cycling were present. The first cluster was driven by *Natrinema* and *Haloterrigena*, while the second cluster was driven by *Gemmatimonas*.

In contrast, inner soils exhibited a stronger statistical potential coupling of the C-N cycles, characterized by a higher number of nodes and links. This complex interaction formed an independent cluster comprising eight pathways (Fig. 5). This cluster was driven by multiple genera of halophilic archaea, including *Halalkalicoccus*, *Halorubrum*, *Halogeometricum*, *Halobacterium*, and *Halomicrobium*. Additionally, a distinct cluster encompassing N-S-coupled pathways, specifically nitrous oxide reduction and sulfur oxidation, was identified in the inner soils, whereas it was notably absent in the outer soils. *Natronorubrum* and *Salinibacter* were primarily associated with these processes within this cluster (Fig. 5). These findings

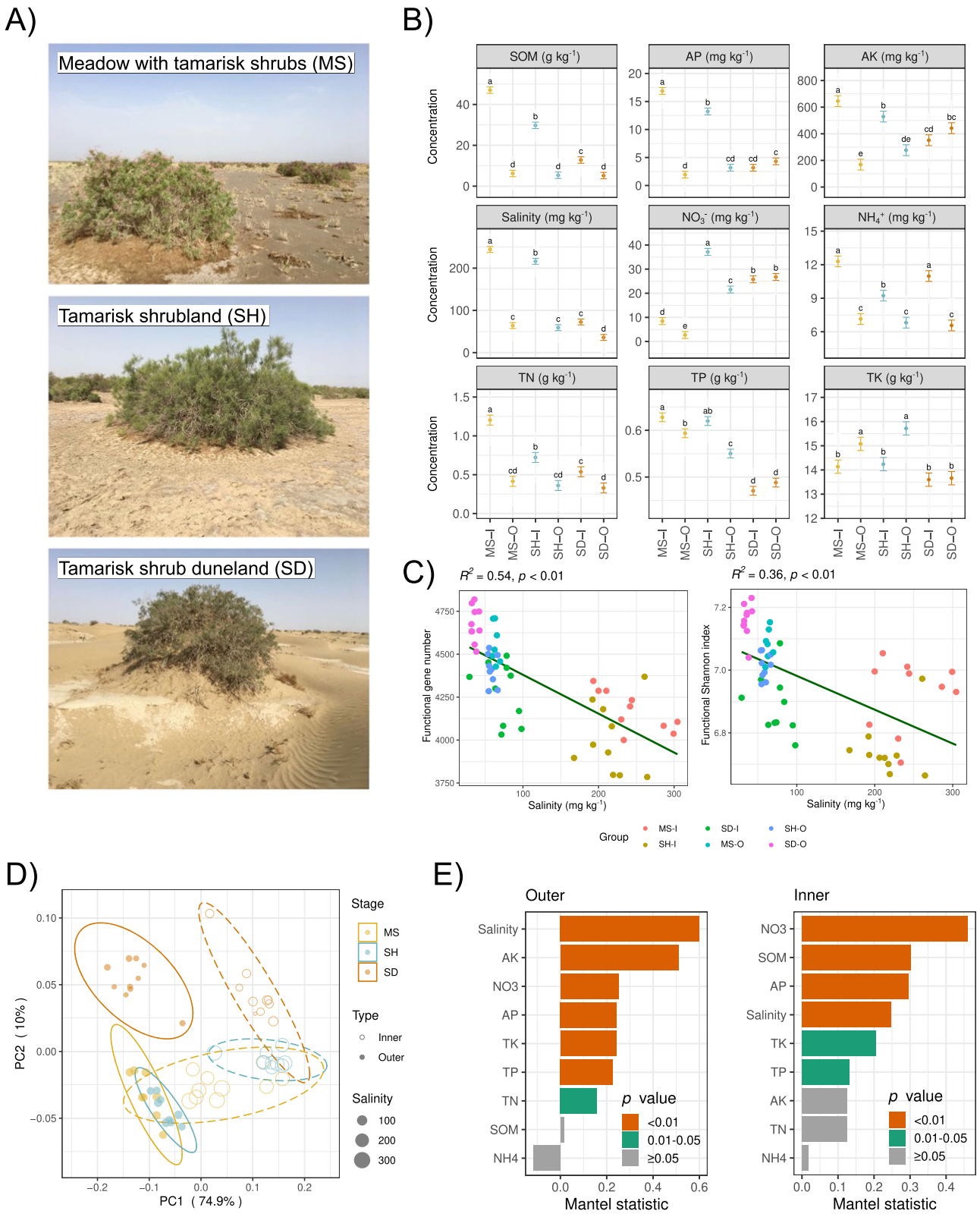

Fig. 1 | Correlation between soil properties and microbial communities. Three arid ecosystems (**A**): "meadow with tamarisk shrubs (MS)", "tamarisk shrubland (SH)", and " tamarisk shrub duneland (SD) ". Comparison of soil properties among different treatments. Significant differences (LSD test, p-value < 0.05) are denoted by distinct lowercase letters. SOM soil organic matter; TN soil total nitrogen, TP soil total phosphorus, TK soil total potassium, AP available phosphorus, AK available potassium (**B**). The influence of salinity on functional alpha-diversity (**C**). Principal coordinates analysis (PCoA) illustrating beta-diversity between different treatments. Hollow points correspond to samples under tamarisk shrubs (inner), while solid points represent samples from the surrounding bare land (outer). The point size represents soil soluble salt content (**D**). Mantel correlation coefficients showing the functional beta diversity correlation with different soil properties. Red indicates p-value < 0.01, green indicates p-value < 0.05, and grey indicates no significant difference (**E**). The error bars display the standard deviation.

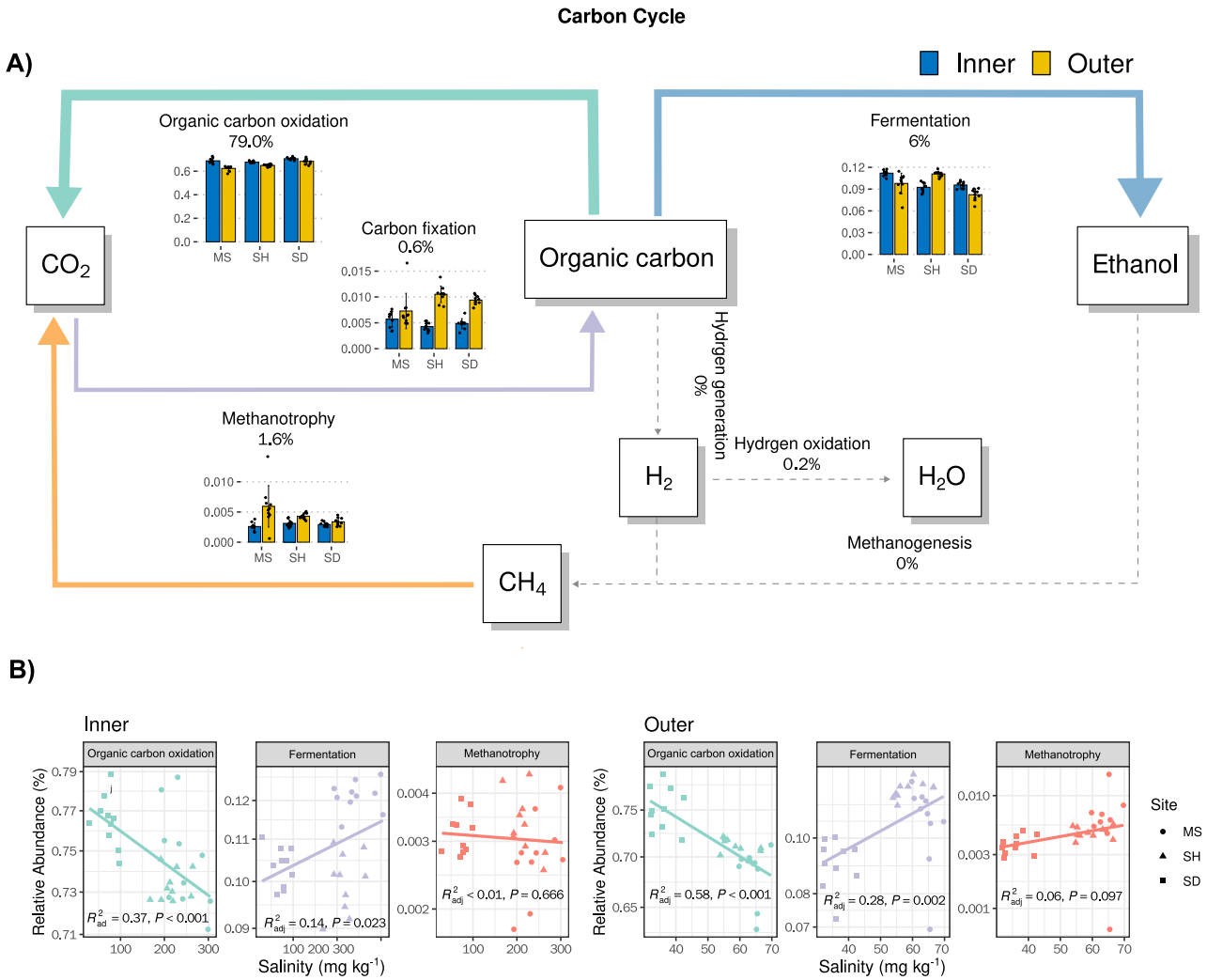

Fig. 2 | Carbon biogeochemical cycle. Line thickness represents the proportion of biomarker genes for the corresponding pathway. Dashed lines indicate proportions lower than 0.1%. Bar plots display the relative abundance of biomarker genes for each pathway (**A**). Spearman's correlations between pathways in the carbon biogeochemical cycle and soil soluble salt content (**B**). The error bars display the standard deviation. MS denotes meadow with tamarisk shrubs, SH denotes tamarisk shrubland, and SD denotes tamarisk shrub duneland. "I" represents soil under tamarisk shrubs (inner), while "O" represents the soil surrounding bare land (outer).

highlight the potential interactions between different biogeochemical cycles and their corresponding taxa in the process of land desertification.

Microbial element-use efficiencies

We conducted tests to assess microbial element-use efficiencies, providing valuable insights into how microbial processes impact mineralization and assimilation across various soil regions. The evaluation of microbial CUE, mineralization, and potential denitrification rates supported our metagenomic findings, indicating elevated activities of carbon and nitrogen cycles within the inner soils (Fig. 6). Microbial CUE and growth rate reached their highest values in the tamarisk shrubland. Notably, microbial CUE and growth rate were significantly lower in the outer soils compared to the inner soils ($p < 0.001$), while respiratory rates were significantly higher in the outer soils than in the inner soils ($p < 0.001$) (Fig. 6). Throughout the three arid ecosystems, it became evident that N mineralization and potential denitrification rates were significantly reduced in the tamarisk shrub duneland compared to the other two ecosystems. Although nitrification showed no significant differences between the inner and outer soils, N mineralization ($p < 0.05$) and denitrification ($p < 0.01$) exhibited marked reductions in the outer soils when compared to the inner soils.

Discussion

Saline terrestrial environments are known for hosting a diverse array of salt-tolerant bacteria and halophilic archaea (haloarchaea), characterized by their unique metabolic diversity, minimal nutritional requirements, and adaptability to saline conditions. Halophytes, prevalent in saline lands, significantly contribute to the elevation of salinity and nutrient levels beneath their canopies, potentially creating a heterogeneous distribution of microorganisms thriving in saline soils. In this study, we pioneered the use of marker genes and isotopic analysis to evaluate microbial ecology patterns and related biochemical processes, providing empirical evidence on soil nutrient cycling in saline environments. Our findings suggests that halophytes may indeed play a pivotal role in regulating soil halophiles and promoting nutrient cycling across distinct arid ecosystems (Fig. 7).

Numerous arid deserts around the world harbor diverse microbial communities, including *Actinobacteria*, *Chloroflexi*, *Proteobacteria*, and *Bacteroidete*[17]. In these arid environments, where clear organic carbon sources are absent, particular members of the *Actinobacteriota* and *Gemmatimonadota* can utilize trace gases as vital energy sources[18,19]. Our current study finds that *Euryarchaeota* (Fig. S3), particularly *Halobacteria*, predominate in soils, likely in response to the prevalent salt stress in three arid ecosystems. Both *Actinobacteriota* and *Gemmatimonadota* were also

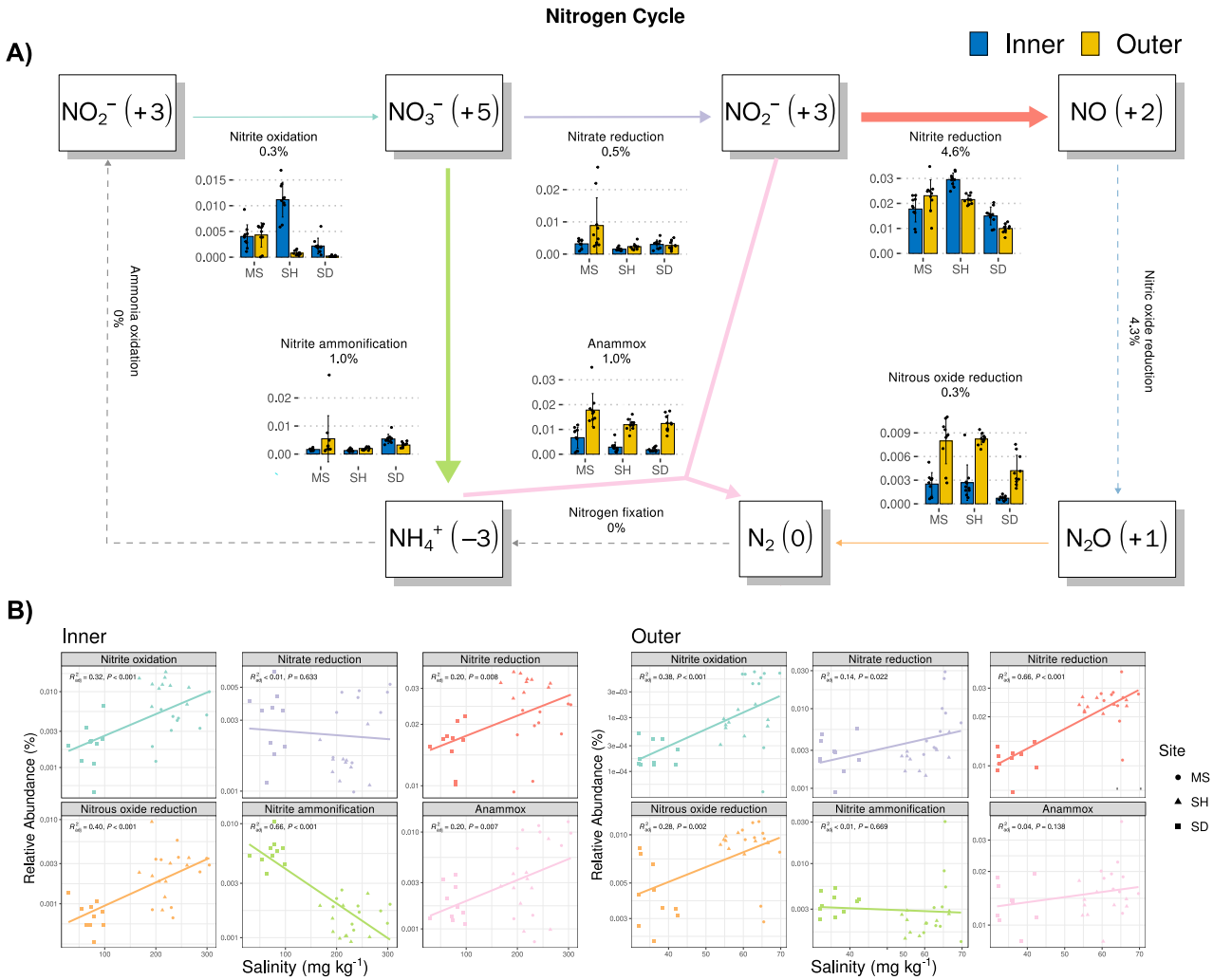

Fig. 3 | Nitrogen biogeochemical cycle. Line thickness indicates the proportion of biomarker genes for each pathway. Dashed lines represent proportions lower than 0.1%. Bar plots depict the relative abundance of biomarker genes for corresponding pathways (**A**). Spearman's correlations between pathways in the nitrogen biogeochemical cycle and soil soluble salt content (**B**). The error bars display the standard deviation. MS represents meadow with tamarisk shrubs, SH represents tamarisk shrubland, and SD represents tamarisk shrub duneland. "I" represents the soil under tamarisk shrubs (inner), and "O" represents the soil surrounding bare land (outer).

commonly found in bare soils (Fig. S3), suggesting that these microbes may employ similar strategies to conserve energy under oligotrophic conditions.

The presence of halophyte-induced saline fertile islands significantly influences composition of soil microbial community and functional genes. Previous studies have underscored the preference of specific taxa, such as *Proteobacteria* and *Actinobacteria*, for soils within plant fertile islands in dryland ecosystem[5,20–22]. In these saline fertile islands, haloarchaea exhibit heightened abundance, and organic matter plays a pivotal role in shaping microbial communities. This finding diverges from earlier studies suggesting that elevated soil salinity may mitigate the impact of soil organic matter on microbiomes[23,24], and that soil pH serves as a reliable indicator for functional gene composition[16].

The observed differences in results may be attributed to the ability of halophiles to actively growth in extreme saline environments, adapting to a wide range of pH conditions from slightly acidic to alkaline[25]. Haloarchaea use the 'salt-in' strategy to maintain osmotic balance, and their enzymes demonstrate remarkable tolerance and higher efficiency in the presence of elevated salt concentrations compared to enzymes of regular microorganisms[26,27]. Additionally, halophilic taxa with a preference for organotrophy may flexibly utilize organic carbon as an energy resource, contributing to their abundance in saline fertile islands. In contrast, halotolerant microbes widely adopt a 'compatible solute strategy' to balance osmotic pressure. This strategy involves maintaining high ATP production to power transmembrane transporters and synthesizing compatible solutes within the cytoplasm—an energetically expensive process[27,28]. These microbes may need to allocate more energy to maintain the physicochemical integrity of their cells in response to changes in salinity, rendering them more sensitive to salinity in bare soils.

The comparison between bare soils and soils beneath the shrub reveals significant disparities in gene abundance and functional potential. In particular, the organic-rich inner soils exhibited higher levels of genes associated with organic carbon oxidation (Fig. 2). This observation aligns with the previous indicating that the greater carbon input can accelerate microbial growth and enzyme activities, ultimately enhancing soil respiration[29]. Among the genes involved in carbon metabolism, those related to pectin metabolism display the most substantial variation in abundance between the bare soils and the inner soils (Fig. S7; Supplementary Data 3). Pectin, a complex polysaccharide found in plant cell walls, is more readily degraded than cellulose[30]. This makes tamarisk litter a readily accessible energy source for heterotrophic microorganisms.

In contrast, resource-poor bare soils exhibit elevated gene levels associated with carbon fixation, H_2 oxidation, methanotrophy, and anammox (Figs. 2, 3). Microbes in such harsh environments have adapted to a low-energy-cost lifestyle, a trait commonly observed in resource-limited settings including carbon-limited bare areas alternating with vegetation patches in drylands[5,31]. These microbes exhibit remarkable efficiency in oxidizing

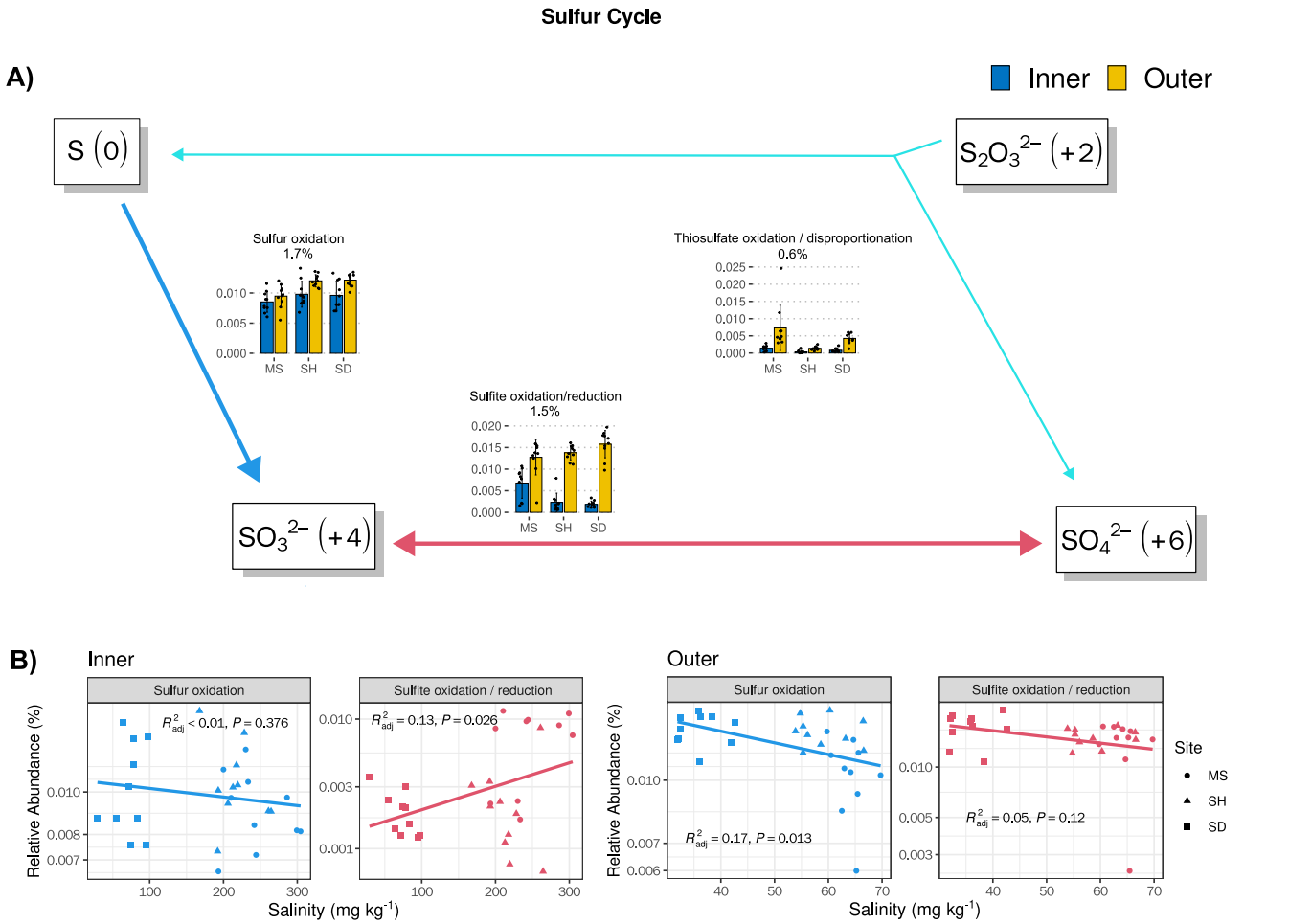

Fig. 4 | Sulfur biogeochemical cycle. Line thickness indicates the proportion of biomarker genes for each pathway. Dashed lines indicate proportions lower than 0.1%. Bar plots show the relative abundance of biomarker genes for corresponding pathways (**A**). Spearman's correlations between pathways in the sulfur biogeochemical cycle and soil soluble salt content (**B**). The error bars display the standard deviation. MS represents meadow with tamarisk shrubs, SH represents tamarisk shrubland, and SD represents tamarisk shrub duneland. "I" represents the soil under tamarisk shrubs (inner), while "O" represents the soil surrounding bare land (outer).

atmospheric trace gases, a vital adaptation for their survival[18,32]. For instance, desert microbes demonstrate the capacity to utilize H_2 as a resource for CO_2 fixation[19,33]. High-affinity methanotrophs, widely distributed across global drylands and inversely correlated with soil organic carbon levels, can effectively utilize atmospheric CH_4 as a carbon source[34]. Additionally, chemolithoautotrophic anammox bacteria have been identified as nitrogen consumers in upland arable soil[35,36]. Anammox bacteria generally exhibit salt tolerance, enabling them to thrive in saline environments[37]. This tolerance may explain the presence of anammox genes in the saline arid ecosystems. In light of these findings, our results suggest that mixotrophic taxa, including autotrophic taxa, are more prevalent in the resource-limited bare soils compared to the resource-abundant shrub islands.

The analysis of function-taxa bipartite networks has revealed associations within nutrients biogeochemical cycles, with the most prominent connections observed between nitrogen and carbon in soils (Fig. 5). Importantly, our results have unveiled those soils in tamarisk islands exhibited a stronger potential carbon-nitrogen cycle compared to bare soils. One compelling example of this enhanced cycle is the observed potential coupling relationship between nitrite or nitric oxide reduction and methanotrophy in inner soils, with such connections being absent in the outer soils. The interconnection between methanotrophy and nitrate reduction has been documented in arid soils, as both processes rely on electron acceptors to sustain microbial metabolism[38]. The decomposition of plant carbon inputs (e.g., litter and dead roots) in desert soils fosters microaerobic conditions or hotspots/hot moments[39–41], while Type II methanotrophs, which thrive near oxic-anoxic interfaces, are prevalent[42]. In this context, the saline fertile islands not only offer essential nutrients for heterotrophic halophilic microbes but also providing an ideal habitat for specific methanotrophic species. This intricate interplay likely contributes to reinforcing the coupling between methanotrophy and nitrite or nitric oxide reduction within the Tamarisk islands.

Furthermore, we observed a distinct interconnection between nitrogen and sulfur cycling in inner soils—an interaction that is absent in the bare soil (Fig. 5). This potential coupling finds its origins in the presence of specific taxa of *Natronorubrum* (as illustrated in Fig. 5), known for their adeptness in utilizing an array of sulfur-containing compounds, including sulfate and sulfide, as potent energy sources for biosynthesis[43]. Such particular taxa potentially serve as the foundational basis for the linkage between nitrogen and sulfur cycling in the islands. Moreover, the soils within these islands exhibited a marked abundance of denitrifying genes compared to the bare soils. Notably, the autotrophic nature of certain denitrifying bacteria, which are endowed with the capability to efficiently exploit thiosulfate as an energy source and nitrate as a terminal electron acceptor[44]. This capacity provides a partial explanation for the intriguing interplay observed between the constituents of nitrogen and sulfur. It is important to note that the potential biogeochemical couplings were inferred from network analysis. To corroborate these findings, additional evidence is necessary, including analyses of metagenome-assembled genomes, complemented by ex-situ measurements of oxidation rates and specific radiolabeled incubation assays.

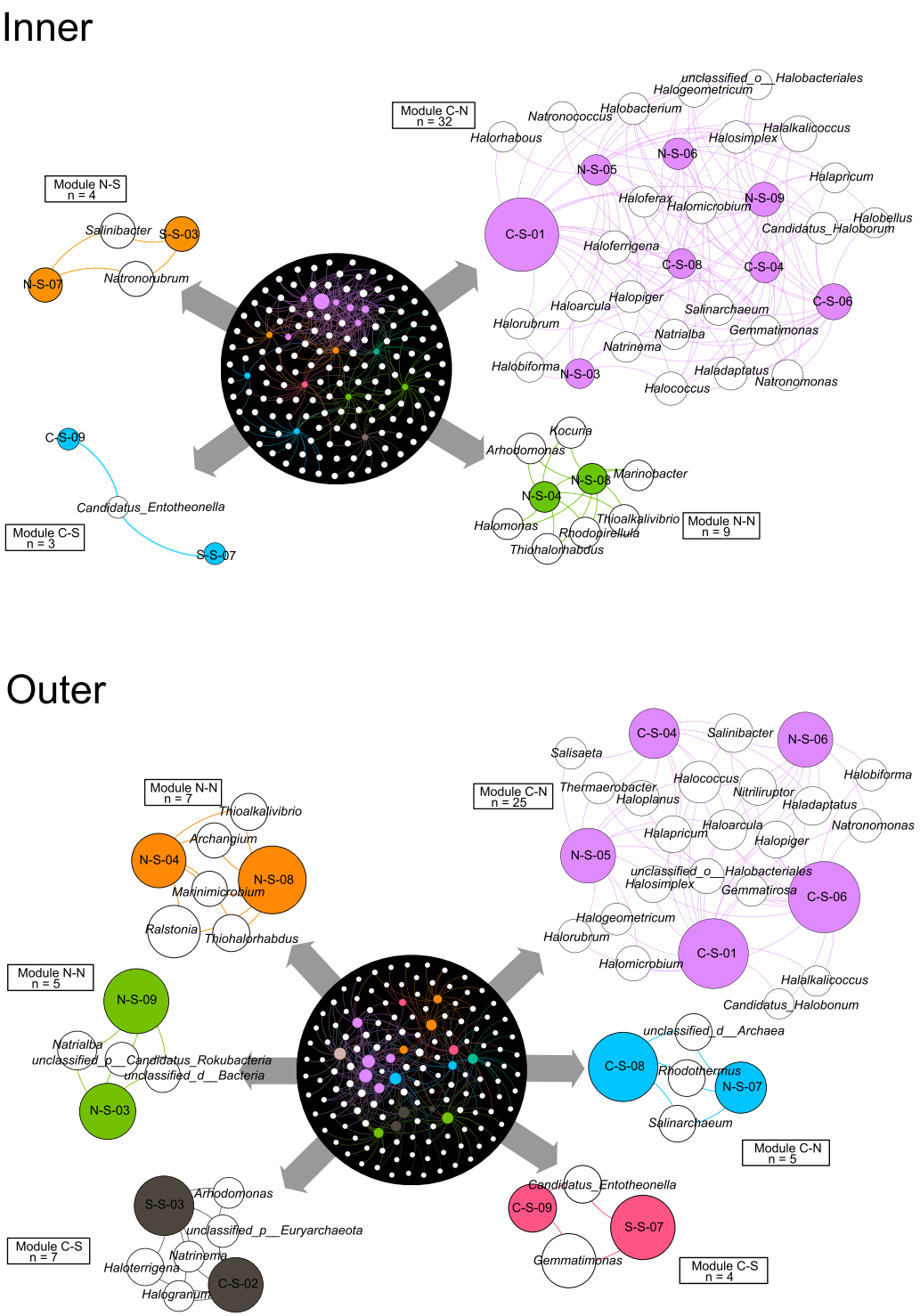

Fig. 5 | Function-taxa bipartite network for biogeochemical cycling processes. Subnetworks derived from functional nodes within each biogeochemical module and their co-associating taxa. Colored circles indicate pathways, colorless circles denote taxa associated with those pathways, and the size of each circle corresponds to relative abundance.

While the predicted potential biogeochemical processes based on metagenomics analysis lack experimental validation, we conducted additional incubation experiments to assess certain processes involved in carbon and nitrogen transformation. Our results unequivocally demonstrated higher microbial carbon use efficiency and growth rate in soils beneath the shrub canopy compared to bare soils (Fig. 6). This increased growth can be attributed to the influx of plant-derived carbon from the shrub, which alleviates resource limitations on microbial growth and creates a positive

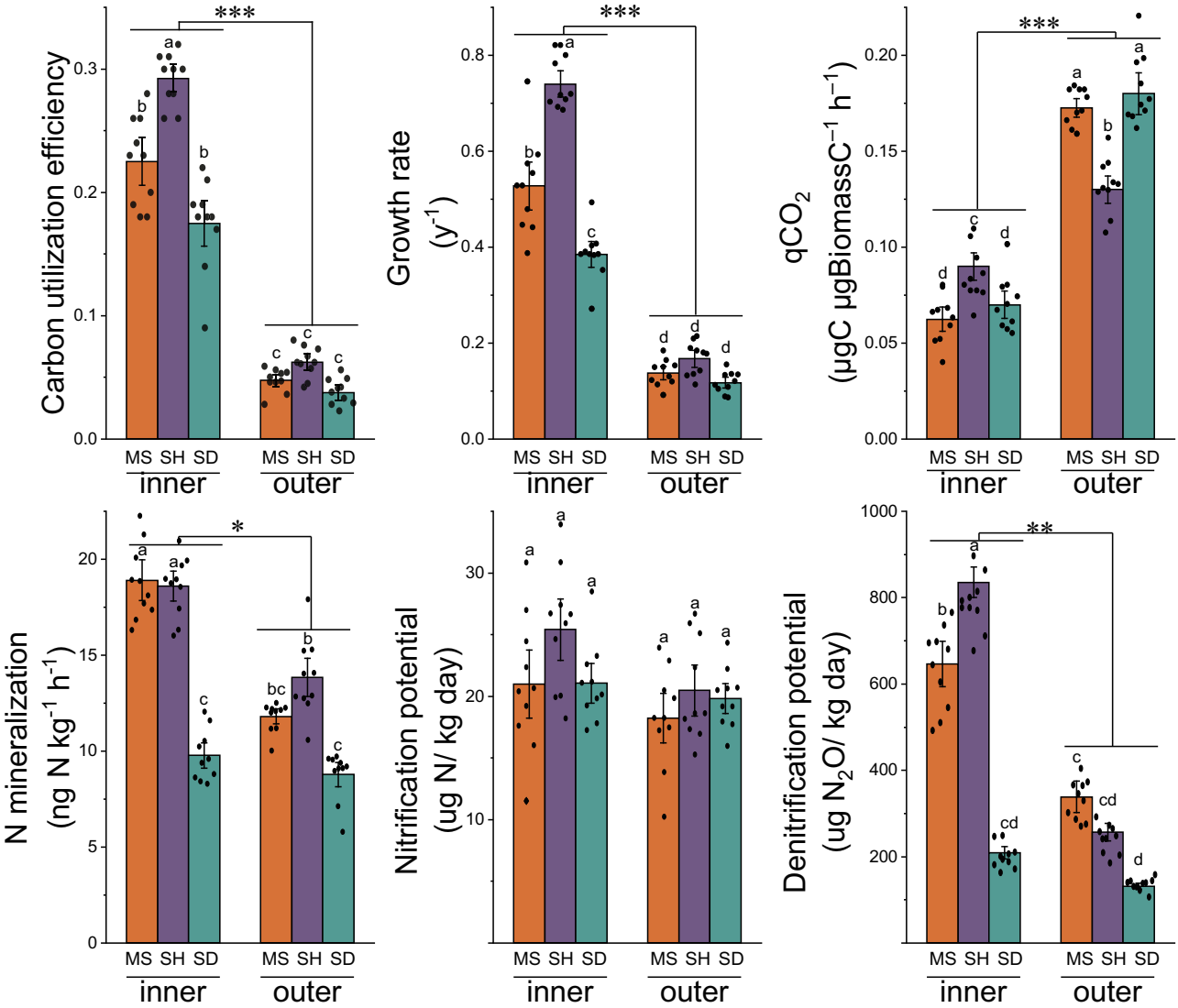

Fig. 6 | Microbial biogeochemical parameters. Comparison of microbial parameters, including carbon utilization efficiency (CUE), growth rate, qCO_2, N mineralization rate, nitrification potential rate, and denitrification potential rate among different treatments. The error bars display the standard deviation. Significant differences (LSD test, p-value < 0.05) are indicated by distinct lowercase letters. All measures show significant differences between the two groups based on Student's t-test, as indicated by asterisks (*$p < 0.05$; **$p < 0.01$, ***$p < 0.001$).

feedback loop that improves microbial growth efficiency[45]. Consequently, the abundant soil organic matter content enhances microbial metabolic processes, thereby intensifying carbon cycling in saline fertile islands. In contrast, microbes in bare soils exhibit limited control over the carbon cycle process, as indicated by their low growth rate. The observed low growth efficiency suggests that microbes allocate a significant portion of their resources and energy toward non-growth maintenance activities[45]. These findings support the theory of physiological trade-offs, which posits that microbial maintenance energy requirements increase in soils depleted of organic resources, resulting in reduced growth efficiency[46]. However, soil microorganisms in bare soils continue to respire, potentially utilizing non-plant carbon sources, such as direct carbon fixation[47]. This finding is consistent with our observation of a higher abundance of carbon fixation genes in bare soils (Fig. 2).

In terms of the nitrogen transformation, we observed a significantly higher rate of N mineralization under shrubs compared to the bare soils (Fig. 6). This heightened mineralization can be attributed to labile carbon inputs from plants, such as leaf litter, which have been shown to stimulate microbial N-mining in subarctic soils[48]. When the stoichiometry of plant inputs closely matches microbial N demand, the surplus N is more likely to undergo mineralization[49].

Our results also indicate higher potential denitrification rates and more pronounced denitrification-derived N_2O production in soils under the shrub canopy (Fig. 6). Previous study suggest that a significant proportion of denitrifying archaea are organotrophic halophiles[50]. Soils with cover crops exhibit elevated denitrifier activity, and specific carbon substrates such as proteins, amino acids, and organic acids can significantly enhance denitrification[51]. Moreover, the application of crop residues with KNO_3 has been found to significantly increase N_2O fluxes compared to other forms of nitrogen[52]. Halophyte-induced saline fertile islands not only have relatively abundant carbon substrates but are also rich in nitrate and potassium ions (Fig. 2). Therefore, we infer that saline-fertile islands create a favorable chemical environment for efficient microbial denitrification, especially for halophilic archaea, which emerging as primary participants in the denitrification process. It should be noted that certain microbiome, such as anammox, participate in denitrification under anaerobic conditions. The increase in soil moisture, potentially due to extreme precipitation, could revive anammox bacteria in arid soils[53,54]. Recent trends have shown increased extreme precipitation events and wetting in the Taklamakan and Gobi Deserts[55], which could boost anammox metabolism in these arid soils. Further studies are necessary to conduct in situ

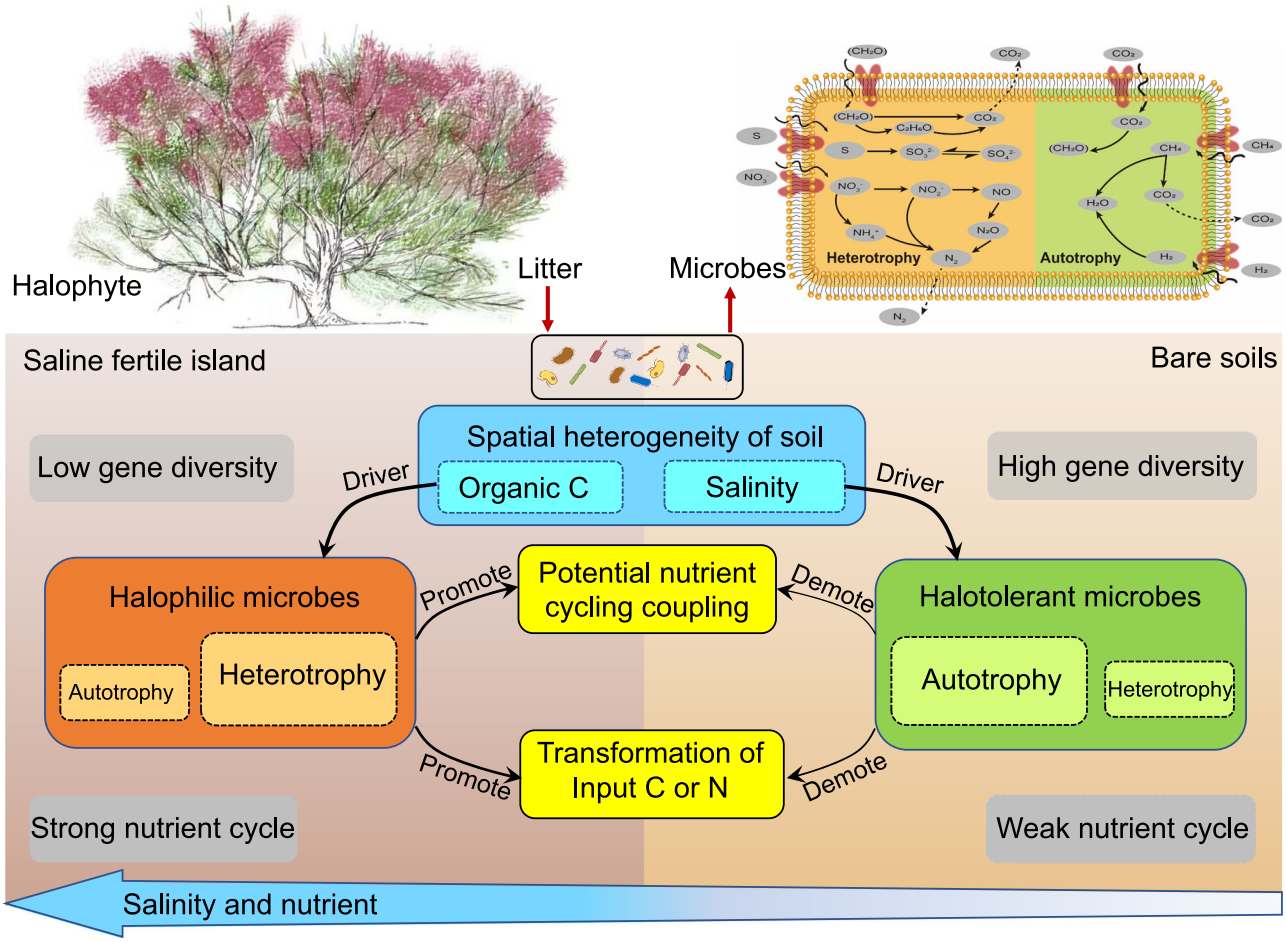

Fig. 7 | Conceptual Infographic: interactions induced by halophyte shrub saline fertile islands across three arid ecosystems. An infographic illustrating the interactions between soil salinity, soil organic carbon, microbial genes, and microbial energy strategies influenced by the presence of saline fertile islands created by halophyte shrubs. The rise in soil salinity and organic C levels, attributed to halophyte shrubs, trigger a shift in microbial groups from halotolerant autotrophic taxa to halophilic heterotrophic taxa. As a result, saline soils within these islands exhibit heightened nutrient cycling compared to bare saline soils.

measurements of denitrification, such as using static chambers, in these arid ecosystems.

Through the isotopic data combined with metagenomic analysis, it unequivocally reveals a substantial enhancement in specific microbial biochemical processes within the saline fertile islands. Notably, numerous microbial processes, such as carbon use efficiency and denitrification, exhibit a pronounced response to variations in climatic factors, thereby influencing the dynamics of soil carbon and nitrogen pools[40,56–59]. The extensive presence of halophytes and their induced islands in arid ecosystems, exemplified by the expansive tamarisk-covered area around Taklamakan exceeding one million hectares[60], underscores the substantial influence of microbiomes in halophyte islands on soil nutrient flows. Subsequent research could unravel the intricate dynamics of halophytes and their associated soil microbiomes, particularly in relation to the storage and stability of soil nutrient pools, against the backdrop of global climate change.

In the saline soils of arid ecosystems, halophyte-induced saline fertile islands significantly contribute to the observed spatial heterogeneity within soil microbial communities. While these saline islands exhibit a reduction in both functional gene alpha-diversity and the relative abundance of most functional genes, they uniquely support specific halophilic microbes with an extensive repertoire of genes associated with carbohydrate, nitrogen, and sulfur utilization. This influence enhances the capacity of halophilic microbes to interconnect essential elements in potential coupling biogeochemical cycles. Conversely, in the bare soils, microorganisms with salt-tolerant adaptations possess an abundance of genes related to carbon fixation, H_2 or CH_4 oxidation, and anaerobic ammonium oxidation. They predominantly rely on autotrophic pathways to thrive in nutrient-poor conditions. These flexible metabolic adaptations allow these microbes to effectively adapt to the highly variable soil conditions, including fluctuations in salinity and nutrient availability. Additionally, in response to nutrient inputs, microbial communities within the islands demonstrate higher carbon use efficiency and enhanced nitrogen translation, signifying their superior ability to efficiently drive nutrient cycling processes. In summary, our findings underscore the central role of halophyte shrubs in shaping biogeochemical dynamics through their profound influence on soil microbial communities in extreme ecosystems.

Methods

Study site description

The study was conducted in September 2021 in three isolated regions located on the alluvial plain in the north marginal zone of the Taklimakan Desert, China. The study sites included three different tamarisk shrub categories: 'meadow with tamarisk shrubs (MS)', 'tamarisk shrubland (SH)', and 'tamarisk shrub duneland (SD)'. Comprehensive information about these categories is provided in Fig. S1. All study sites share the same climate conditions, characterized by extremely low precipitation, with mean annual precipitation varying from 53.3 to 77.5 mm, and very high evaporation, with mean annual potential evaporation varying from 2750 to 3532 mm[9].

Soil sampling

To ensure a comprehensive assessment of the soil microbiome in the study area, a total of 30 plots (120 × 120 m) were established, with ten plots for

each site (Fig. S1). From each plot, ten living tamarisk shrubs were selected, and ten soil cores (0–20 cm) beneath each canopy were collected and mixed to obtain one composite sample. To serve as controls, three soil cores (0–20 cm) were harvested from the bare land around each canopy in each plot, and 30 cores were mixed to obtain one composite sample in each plot, following Yin's protocol[9]. In total, 60 soil samples were collected, representing the microbiome of the soil under tamarisk shrubs (inner), and the surrounding bare land (outer). The composited soil samples were sieved through a 2 mm mesh to remove plant residues and stones. A portion of each soil sample was placed in a sealed plastic bag, immediately transferred to the laboratory using a cooler box, and stored at −80 °C until soil DNA extraction was carried out. The remaining soils were tested for their physicochemical properties.

Soil physicochemical property determination

The edaphic variables were measured following the methods previously described[61]. To provide a brief overview, the soil soluble salt content of the soil samples was determined by measuring the residue post-drying. Available phosphorus was quantified employing a spectrophotometer (UVmini-1240, Shimadzu, Japan), while available potassium was measured using an atomic absorption spectrum analyzer (240-AA, Agilent, USA). Soil pH was measured using a pH meter after shaking a soil/water suspension (1:5, w/v). Soil organic matter was ascertained through colorimetry subsequent to oxidation with a potassium dichromate and sulfuric acid mixture. Concentrations of total, NH_4^+-N and NO_3^--N were determined using a Kjeldahl nitrogen analyzer (Kjeltec 8460, Foss, USA). Ion concentrations were detected using inductively coupled plasma mass spectrometry (ELAN 9000/DRC-e, PerkinElmer, USA). The physicochemical properties of all the soil samples are shown in Supplementary Data 7.

Incubation experiment

For microbial basal respiration measurements, an aliquot (5 g) of the field-moist soil was placed into a 50 mL glass vial and incubated overnight in the dark at room temperature (24 °C) without manipulating the moisture levels. Respired CO_2 collected in the headspace was measured using a gas chromatography isotope ratio mass spectrometer (GC-IRMS, Delta-V, Thermo Fisher Scientific, Germany). Following the procedure, vials with soils were opened and incubated in the dark for 8 h before adding 100 μL of ^{13}C-labeled DOC solution (0.13 mg C). The filter-sterilized solution was prepared from ^{13}C-labeled powdered Maize (*Zea mays*) leaf (97 atom% ^{13}C), containing a range of compounds varying in their decomposability (Shanghai ZZBIO Co., Ltd., China). Respiration measurements were repeated following the same incubation procedure as mentioned above to obtain the proportion of DO^{13}C in respired CO_2.

Soil DNA extraction was carried out on a soil aliquot of 0.25 g using DNA isolation kit. Since soil microbial DNA is a strong indicator of soil microbial biomass carbon in arid ecosystems[62], in this study we estimated soil microbial biomass carbon using soil microbial DNA without applying any correction between them. Another set of identical DNA extraction was performed following addition of 50 μL of DO^{13}C solution and overnight incubation in the dark at field moisture capacity. Both extracts were analyzed in the HPLC system coupled to a Delta - V IRMS. This allowed us to obtain the DNA-C content and the proportion of DO^{13}C in microbial DNA from soils with and without substrate addition. Microbial carbon utilization efficiency (CUE) was estimated as DNA-^{13}C/ (DNA-^{13}C + $\sum CO_2$-^{13}C), where $\sum CO_2$-^{13}C is the cumulative DO^{13}C lost during respiration[45]. Microbial growth rate was calculated as DNA- ^{13} C/DNA-C.

Soil microbial gross N mineralization was estimated using modified ^{15}N isotope dilution methods described by Hart et al. [63]. Duplicate of 20 g moist soil samples were added into 200 mL glass cups covered with pierced Para-film and pre-incubated at 24 °C for 24 h, then evenly dropwise labeled with 1 ml $^{15}NH_4Cl$ (10 atom% ^{15}N), and the cups were incubated at 24 °C. For the determination of NH_4^+-N, soils were extracted immediately, as well as 2 days and 7 days after labeling, by suspension in 100 mL of 2 M KCl solution for 1 h on a shaker. The NH_4^+-N content was then measured using a continuous flow analyzer. Subsequently, the N isotope ratio of NH_4^+-N was measured using the ammonium diffusion method and analyzed with a Delta-V IRMS. The gross rates were calculated using the equation developed by Kirkham and Bartholomew.

The soil nitrification potential was determined following the protocol described by Drury et al. [64]. In brief, a total of 10 grams of freshly sieved soil (mesh size: 4 mm) was weighed into a 250 mL Schott bottle. Subsequently, 100 mL of a freshly prepared NH_4^+ nutrient solution with a pH of 7.2 (containing 1.5 mM NH_4^+ and 1 mM PO_4^{3-}) was added to the soil. The samples were then shaken at 130 rpm under 24 °C. At designated time points (2, 4, 24, 48, and 72 h), 10 mL of the solution was collected from each replicate to measure the rate of potential nitrification. The collected solution was centrifuged at 4600 rpm for 10 min and subsequently filtered using a 0.45 μm syringe filter. The supernatant samples were immediately stored at −20 °C until analysis. Concentrations of NH_4^+-N and NO_3^--N were determined using Continuous Flow Analyzer (AA3, Seal, Germany).

Potential denitrification activity was performed as a proxy of concentration of denitrifying enzymes in a soil sample[65]. Two assays were conducted for each soil sample: one with acetylene to measure the overall denitrification potential, and one without acetylene to measure N_2O formation. For both assays, 20 grams of moist soil were immersed in 30 mL of solution containing 1 mM KNO_3, 0.5 mM glucose, 0.5 mM sodium acetate and 0.5 mM sodium succinate in 100 mL glass bottle with rubber stopper. The bottle was flushed with N_2 for 3 min and then was vented to reach atmospheric pressure. After 15 mL of acetylene was added, the bottles were shaken at 100 rpm for three hours and gas samples was collected at 60, 90, 120, 180 min. Gas samples were analyzed using a Gas Chromatograph (6890 N, Agilent Technologies, USA) equipped with an electron capture detector. Rates of denitrification potential and N_2O formation were calculated using the slope of the linear regression model based on the four time points for each set of samples.

DNA extraction and metagenomic sequencing

Soil DNA was extracted using FastDNA® SPIN Kit for Soil (MP Biomedicals, USA). The quantity of the DNA was measured by a Qubit 4.0 fluorometer (Invitrogen, USA). The soil DNA purity was performed by absorption ratio of A260/280 using a NanoDrop 2000 spectrophotometer (Thermo Scientific, USA). Soil DNA was fragmented to an average length of approximately 300 bp with Covaris M220 following the recommended instructions, to construct a PE library with a read length of 150 bp. The PE sequencing was performed on the Illumina Hiseq X ten system (Illumina Inc., San Diego, CA, USA) at Shanghai Majorbio Bio-pharm Technology Co., Ltd., using HiSeq 3000/4000 PE Cluster Kit and SBS Kits.

The metagenomic data analysis was conducted using previously described methods[41], and the basic metagenomic sequencing information is shown in Supplementary Data 8. Briefly, the quality control of the paired-end reads was processed with Fastp (ver. 0.20.0, https://github.com/OpenGene/fastp), to remove the adapter sequences. Low-quality reads with sequence length <100 bp, an average quality score <20, and having ambiguous N bases, were filtered with Sickle software version 1.33 (https://github.com/najoshi/sickle). Clean reads were assembled into contigs (a total of 62,358,190 contigs with an N50 value of 770 bp) using Megahit v1.1.2 (http://www.l3-bioinfo.com/products/megahit.html). After the quality control, shotgun sequencing generated 84.8 ± 7.8 million sequences, or 12.6 ± 1.2 Gbps of sequencing effort, and 83.8 ± 7.7 million sequences remained for downstream analysis.

Gene prediction, taxonomy and functional annotation

The open reading frames (ORFs) of contigs were predicted for gene prediction using MetaGene (http://metagene.cb.k.u-tokyo.ac.jp/). The ORFs were used to construct a non-redundant gene catalog with CD-HIT, applying criteria of 95% sequence identity and 90% coverage. For community profiling, ribosomal RNAs (rRNAs) were identified using the nhmmer function, part of HMMER3, from Barrnap (v0.9) (https://github.com/tseemann/barrnap). The options '-reject 0.01 -e-value 1e-3' and

'-kingdom bac/arc' were used for bacteria (5S, 23S, and 16S rRNA genes) and archaea (5S, 5.8S, 23S, and 16S rRNA genes), respectively. For gene taxonomic annotation, the non-redundant gene catalog was searched against the NR (Non-Redundant Protein Sequence) database using Diamond with the best-hit method and an e-value threshold of 1e-5. For gene functional annotation, the predicted ORFs were analyzed by Diamond against the KEGG (Kyoto Encyclopedia of Genes and Genomes) database, also using the best-hit method with an e-value threshold of 1e-5.

We specifically annotated genes associated with the carbon (C), nitrogen (N), and sulfur (S) cycles using the METABOLIC tool. Read counts of functional genes in each sample were mapped to the gene catalog using SOAPaligner v2.2.1 (http://soap.genomics.org.cn/soapaligner.html), and the number of reads corresponding to functional genes in each sample was calculated. Information on the selected functional genes is provided in Supplementary Data 2. The relative abundance of taxon and functional genes was calculated by summing the number of reads assigned to that taxon/function, and then divided the corresponding read counts by the total read count of the subject. In addition, the coverage profiles of each sample were merged into an abundance matrix for a corresponding CPM (Counts Per Million–normalized) using a TMM (Trimmed Mean of M values) method[66], which takes into account both relative size of metagenomes and library sizes.

Statistics and reproducibility

Differences in soil characteristics, N cycling rates, Potential denitrification activity, N_2O formation, respiration and the relative abundance of functional genes involved in C, N, P, and S cycling between treatments were evaluated by the Wilcoxon rank-sum test with 95% confidence intervals, and a p-value lower than 0.05 was considered to be significant.

The library was rarefied to match the smallest sample size. For each sample, the proportion of unannotated genes was determined by dividing the number of genes without KEGG annotations by the total number of genes. Functional gene diversity was assessed using the Shannon-Weiner diversity index 'H', and gene richness was measured using the number of functional genes found in corresponding samples. Functional composition dissimilarity was analyzed using Bray-Curtis dissimilarity and visualized using principal coordinate analysis (PCoA), and distance-based redundancy analysis (dbRDA) were conducted using the R 'vegan' package[67]. PERMANOVA (Permutational Multivariate Analysis of Variance), as described by Anderson in 2017[68], was employed to assess the impact of soil variables on the composition of functional genes. To evaluate the correlations between soil physicochemical properties and functional gene compositions, we conducted a Mantel test.

We constructed a Spearman's correlation matrix to analyze the relationships among functional genes based on their relative abundances in each soil sample. To reduce potential bias in correlation coefficients, we utilized the functional gene abundance matrix in Counts Per Million and retained only those functional genes present in more than half (> 50%) of all soil samples, following the approach outlined by Liu et al. in 2023[41]. Subsequently, we conducted function-taxon bipartite network analysis to investigate the associations between biomarker functional genes and their corresponding microbial taxa. This analysis integrated the functional profiles and taxonomy of contigs assembled from the metagenomes using the 'ggraph' package. In the resulting network, individual nodes represented functional genes, while edges represented significant correlations, characterized by robust Spearman's coefficients (rho) exceeding 0.6 and FDR-corrected p-values less than 0.01, as detailed by Ma et al. [69].

Data availability

The metagenomic sequencing dataset that support the findings of this study are openly available in the National Center for Biotechnology Information (NCBI) Sequence Read Archive (SRA) database with accession number PRJNA1035643 at https://www.ncbi.nlm.nih.gov/sra. The source data for Fig. 1 is available in Supplementary Data 7 and Supplementary Data 9. The relative abundance of biomarker genes underlying Figs. 2, 3, and 4 is provided in Supplementary Data 10. The source data for the graphs in Fig. 5 can be found in Supplementary Data 11, while all source data for Fig. 6 is included in Supplementary Data 12. Any additional data from this study are available upon request.

Received: 22 March 2024; Accepted: 16 August 2024;
Published online: 29 August 2024

References

1. Coban, O., De Deyn, G. B. & van der Ploeg, M. Soil microbiota as game-changers in restoration of degraded lands. *Science* **375**, abe0725 (2022).
2. Hakobyan, A. et al. Tillandsia landbeckii phyllosphere and laimosphere as refugia for bacterial life in a hyperarid desert environment. *Microbiome* **11**, 246 (2023).
3. Gao, Y. et al. "Fertile islands" beneath three desert vegetation on soil phosphorus fractions, enzymatic activities, and microbial biomass in the desert-oasis transition zone. *CATENA* **212**, 106090 (2022).
4. Jones, D. L. et al. Life at the extreme: Plant-driven hotspots of soil nutrient cycling in the hyper-arid core of the Atacama Desert. *Soil Biol. Biochem.* **184**, 109128 (2023).
5. Li, S. et al. Reduced trace gas oxidizers as a response to organic carbon availability linked to oligotrophs in desert fertile islands. *ISME J.* **17**, 1257–1266 (2023).
6. Marlin, D., Newete, S. W., Mayonde, S. G., Smit, E. R. & Byrne, M. J. Invasive Tamarix (Tamaricaceae) in South Africa: current research and the potential for biological control. *Biol. Invasions* **19**, 2971–2992 (2017).
7. Lesica, P. & DeLuca, T. H. Is tamarisk allelopathic? *Plant Soil* **267**, 357–365 (2004).
8. Ladenburger, C. G., Hild, A. L., Kazmer, D. J. & Munn, L. C. Soil salinity patterns in Tamarix invasions in the Bighorn Basin, Wyoming, USA. *J. Arid Environ.* **65**, 111–128 (2006).
9. Yin, C. et al. The role of tamarisk in the spatial heterogeneity of soil resources in the northern Tarim Basin, Xinjiang, China. *Plant Soil* **420**, 523–538 (2017).
10. Lozupone, C. A. & Knight, R. Global patterns in bacterial diversity. *Proc. Natl Acad. Sci.* **104**, 11436–11440 (2007).
11. Singh, K. Microbial and Enzyme Activities of Saline and Sodic Soils. *Land Degrad. Dev.* **27**, 706–718 (2016).
12. DeVilbiss, S. E., Taylor, J. M. & Hicks, M. Salinization and sedimentation drive contrasting assembly mechanisms of planktonic and sediment-bound bacterial communities in agricultural streams. *Glob. Change Biol.* **29**, 5615–5633 (2023).
13. Orphan, V. J., House, C. H., Hinrichs, K.-U., McKeegan, K. D. & DeLong, E. F. Methane-Consuming Archaea Revealed by Directly Coupled Isotopic and Phylogenetic Analysis. *Science* **293**, 484–487 (2001).
14. Hallam, S. J. et al. Reverse Methanogenesis: Testing the Hypothesis with Environmental Genomics. *Science* **305**, 1457–1462 (2004).
15. Anantharaman, K., Breier, J. A. & Dick, G. J. Metagenomic resolution of microbial functions in deep-sea hydrothermal plumes across the Eastern Lau Spreading Center. *ISME J.* **10**, 225–239 (2016).
16. Ma, B. et al. Soil Biogeochemical Cycle Couplings Inferred from a Function-Taxon Network. *Research* **2021**, 7102769 (2021).
17. Bay, S. et al. Life without water: how do bacteria generate biomass in desert ecosystems? *Microbiol Aust.* **39**, 28–32 (2018).
18. Bay, S. K. et al. Trace gas oxidizers are widespread and active members of soil microbial communities. *Nat. Microbiol.* **6**, 246–256 (2021).
19. Bay, S. K. et al. Chemosynthetic and photosynthetic bacteria contribute differentially to primary production across a steep desert aridity gradient. *ISME J.* **25**, 3339–3356 (2021).
20. Sun, Y. et al. Effects of xeric shrubs on soil microbial communities in a desert in northern China. *Plant Soil* **414**, 281–294 (2017).
21. Xiang, X. et al. Shrub encroachment is associated with changes in soil bacterial community composition in a temperate grassland ecosystem. *Plant Soil* **425**, 539–551 (2018).
22. Li, S. et al. Fertile islands lead to more conspicuous spatial heterogeneity of bacteria than soil physicochemical properties in a desert ecosystem. *CATENA* **206**, 105526 (2021).

23. Dong, Y. et al. Interactive effects of salinity and SOM on the ecoenzymatic activities across coastal soils subjected to a saline gradient. *Geoderma* **406**, 115519 (2022).
24. Jia, J. et al. Relationships between soil biodiversity and multifunctionality in croplands depend on salinity and organic matter. *Geoderma* **429**, 116273 (2023).
25. Oren, A., Arahal, D. R. & Ventosa, A. Emended descriptions of genera of the family Halobacteriaceae. *Int. J. Syst. Evol. Microbiol.* **59**, 637–642 (2009).
26. Kumar, V. et al. Halocins, natural antimicrobials of Archaea: Exotic or special or both? *Biotechnol. Adv.* **53**, 107834 (2021).
27. Li, J., Gao, Y., Dong, H. & Sheng, G. P. Haloarchaea, excellent candidates for removing pollutants from hypersaline wastewater. *Trends Biotechnol.* **40**, 226–239 (2022).
28. Mokashe, N., Chaudhari, B. & Patil, U. Operative utility of salt-stable proteases of halophilic and halotolerant bacteria in the biotechnology sector. *Int. J. Biol. Macromol.* **117**, 493–522 (2018).
29. Kuzyakov, Y., Horwath, W. R., Dorodnikov, M. & Blagodatskaya, E. Review and synthesis of the effects of elevated atmospheric CO2 on soil processes: No changes in pools, but increased fluxes and accelerated cycles. *Soil Biol. Biochem.* **128**, 66–78 (2019).
30. Du, J., Anderson, C. T. & Xiao, C. Dynamics of pectic homogalacturonan in cellular morphogenesis and adhesion, wall integrity sensing and plant development. *Nat. Plants* **8**, 332–340 (2022).
31. Chen, Y., Neilson, J. W., Kushwaha, P., Maier, R. M. & Barberán, A. Life-history strategies of soil microbial communities in an arid ecosystem. *ISME J.* **15**, 649–657 (2021).
32. Greening, C. & Grinter, R. Microbial oxidation of atmospheric trace gases. *Nat. Rev. Microbiol.* **20**, 513–528 (2022).
33. Ji, M. et al. Atmospheric trace gases support primary production in Antarctic desert surface soil. *Nature* **552**, 400–403 (2017).
34. Lafuente, A. et al. Global drivers of methane oxidation and denitrifying gene distribution in drylands. *Glob. Ecol. Biogeogr.* **28**, 1230–1243 (2019).
35. Shen, L., Wu, H., Liu, X. & Li, J. Vertical distribution and activity of anaerobic ammonium-oxidising bacteria in a vegetable field. *Geoderma* **288**, 56–63 (2017).
36. Nie, S., Zhu, G. B., Singh, B. & Zhu, Y. G. Anaerobic ammonium oxidation in agricultural soils-synthesis and prospective. *Environ. Pollut.* **244**, 127–134 (2019).
37. Zhang, G. et al. Microbial diversity and functions in saline soils: A review from a biogeochemical perspective. *J. Adv. Res.* **59**, 129–140 (2024).
38. Bodelier, P. L. E., Pérez, G., Veraart, A. J. & Krause, S. M. B. Methanotroph Ecology, Environmental Distribution and Functioning. in *Methanotrophs: Microbiology Fundamentals and Biotechnological Applications* (ed. Lee, E. Y.) 1–38 (2019).
39. Tian, J. et al. Soil organic matter availability and climate drive latitudinal patterns in bacterial diversity from tropical to cold temperate forests. *Funct. Ecol.* **32**, 61–70 (2018).
40. Dai, Z. et al. Elevated temperature shifts soil N cycling from microbial immobilization to enhanced mineralization, nitrification and denitrification across global terrestrial ecosystems. *Glob. Change Biol.* **26**, 5267–5276 (2020).
41. Liu, J. et al. Conversion of steppe to cropland increases spatial heterogeneity of soil functional genes. *ISME J.* **17**, 1872–1883 (2023).
42. Wendy, H. et al. Global gases. In Principles and Applications of Soil Microbiology. Elsevier. 557–579 (2021).
43. Venceslau, S. S., Stockdreher, Y., Dahl, C. & Pereira, I. A. C. The "bacterial heterodisulfide" DsrC is a key protein in dissimilatory sulfur metabolism. *Biochim. Biophys. Acta BBA - Bioenerg.* **1837**, 1148–1164 (2014).
44. Monachon, M., Albelda-Berenguer, M. & Joseph, E. Chapter One - Biological oxidation of iron sulfides. in *Advances in Applied Microbiology* (eds. Gadd, G. M. & Sariaslani, S.). **107**, 1–27 (2019).
45. Malik, A. A. et al. Land use driven change in soil pH affects microbial carbon cycling processes. *Nat. Commun.* **9**, 3591 (2018).
46. Manzoni, S., Taylor, P., Richter, A., Porporato, A. & Ågren, G. I. Environmental and stoichiometric controls on microbial carbon-use efficiency in soils. *N. Phytol.* **196**, 79–91 (2012).
47. Malik, A. A., Thomson, B. C., Whiteley, A. S., Bailey, M. & Griffiths, R. I. Bacterial Physiological Adaptations to Contrasting Edaphic Conditions Identified Using Landscape Scale Metagenomics. *mBio* **8**, e00799–17 (2017).
48. Na, M., Yuan, M., Hicks, L. C. & Rousk, J. Testing the environmental controls of microbial nitrogen-mining induced by semi-continuous labile carbon additions in the subarctic. *Soil Biol. Biochem.* **166**, 108562 (2022).
49. Lavallee, J. M., Soong, J. L. & Cotrufo, M. F. Conceptualizing soil organic matter into particulate and mineral-associated forms to address global change in the 21st century. *Glob. Change Biol.* **26**, 261–273 (2020).
50. Offre, P., Spang, A. & Schleper, C. Archaea in biogeochemical cycles. *Annu. Rev. Microbiol.* **67**, 437–457 (2013).
51. Curtright, A. J. & Tiemann, L. K. Chemical identity of carbon substrates drives differences in denitrification and N2O reduction within agricultural soils. *Soil Biol. Biochem.* **184**, 109078 (2023).
52. Xiao, Y. et al. Influence of winter crop residue and nitrogen form on greenhouse gas emissions from acidic paddy soil. *Eur. J. Soil Biol.* **85**, 23–29 (2018).
53. Zhu, G. et al. Resuscitation of anammox bacteria after > 10,000 years of dormancy. *ISME J.* **13**, 1098–1109 (2019).
54. Hu, S. et al. Hydrothermal conditions determine soil potential net N mineralization rates in arid and semi-arid grasslands. *Funct. Ecol.* **36**, 2626–2635 (2022).
55. Dong, W. et al. Recent wetting trend over Taklamakan and Gobi Desert dominated by internal variability. *Nat. Commun.* **15**, 4379 (2024).
56. Ding, X. et al. Warming increases microbial residue contribution to soil organic carbon in an alpine meadow. *Soil Biol. Biochem.* **135**, 13–19 (2019).
57. Naylor, D. et al. Soil Microbiomes Under Climate Change and Implications for Carbon Cycling. *Annu. Rev. Environ. Resour.* **45**, 29–59 (2020).
58. Séneca, J. et al. Increased microbial expression of organic nitrogen cycling genes in long-term warmed grassland soils. *ISME Commun.* **1**, 1–9 (2021).
59. Wu, D. et al. Microbial potential for denitrification in the hyperarid Atacama Desert soils. *Soil Biol. Biochem.* **157**, 108248 (2021).
60. Yang, W., Zhang, D., Yin, L. & Zhang, L. Distribution and cluster analysis on the similarity of the tamarix communities in Xinjiang (In chinese). *Arid Zone Res*. **19**, 6–11 (2002).
61. Zhao, S. et al. Biogeographical distribution of bacterial communities in saline agricultural soil. *Geoderma* **361**, 114095 (2020).
62. Gong, H. et al. Soil microbial DNA concentration is a powerful indicator for estimating soil microbial biomass C and N across arid and semi-arid regions in northern China. *Appl Soil Ecol.* **160**, 103869 (2021).
63. Hart, S. C. et al. Dynamics of gross nitrogen transformations in an old-growth forest: the carbon connection. *Ecology* **75**, 880–891 (1994).
64. Drury, C. F. et al. Nitrification techniques for soils. In: Canadian Society of Soil Science (Ed.), Soil Sampling and Methods of Analysis, second ed. Taylor & Francis, 495–513 (2008).
65. Smith, M. S., Firestone, M. K. & Tiedje, J. M. The Acetylene Inhibition Method for Short-term Measurement of Soil Denitrification and its Evaluation Using Nitrogen-13. *Soil Sci. Soc. Am. J.* **42**, 611–615 (1978).
66. Robinson, M. D. & Oshlack, A. A scaling normalization method for differential expression analysis of RNA-seq data. *Genome Biol.* **11**, R25 (2010).
67. Oksanen, J. et al. "vegan: community ecology package," R package http://www.CRAN.R-project.org/package=vegan (2019).
68. Anderson, M. J. Permutational Multivariate Analysis of Variance (PERMANOVA), in: Wiley StatsRef: Statistics Reference Online. John Wiley & Sons, Ltd, 1–15 (2017).

69. Ma, B. et al. Genetic correlation network prediction of forest soil microbial functional organization. *ISME J.* **12**, 2492–2505 (2018).

Acknowledgements
This work was supported by the National Natural Science Foundation of China (31470713 and 31971448), the Youth Innovation Promotion Association CAS (grant no. 2020433), and Natural Science Foundation of Heilongjiang Province (ZD2022D001). We thank the editor and reviewers for their constructive suggestions and insightful comments.

Author contributions
S.Z. and J.L. conceived the study; S.Z., C.Y. and B.P. managed the field site, developed the lab methodology, conducted the lab work and collected samples; H.G. and N.Z. analyzed the data and interpreted the findings with X.L., B.W and C.T.; M.G.A.H. and S.B. commented on the text and contributed to the interpretation of the results. S.Z. and J.L. wrote the manuscript with input from all authors.

Competing interests
The authors declare no competing interests.

Additional information
Supplementary information The online version contains supplementary material available at https://doi.org/10.1038/s42003-024-06741-1.

Correspondence and requests for materials should be addressed to Jun-jie Liu or Chuan-hua Yin.

Peer review information *Communications Biology* thanks the anonymous reviewers for their contribution to the peer review of this work. Primary Handling Editor: Luke Grinham. A peer review file is available.

Reprints and permissions information is available at http://www.nature.com/reprints

Publisher's note Springer Nature remains neutral with regard to jurisdictional claims in published maps and institutional affiliations.

Open Access This article is licensed under a Creative Commons Attribution-NonCommercial-NoDerivatives 4.0 International License, which permits any non-commercial use, sharing, distribution and reproduction in any medium or format, as long as you give appropriate credit to the original author(s) and the source, provide a link to the Creative Commons licence, and indicate if you modified the licensed material. You do not have permission under this licence to share adapted material derived from this article or parts of it. The images or other third party material in this article are included in the article's Creative Commons licence, unless indicated otherwise in a credit line to the material. If material is not included in the article's Creative Commons licence and your intended use is not permitted by statutory regulation or exceeds the permitted use, you will need to obtain permission directly from the copyright holder. To view a copy of this licence, visit http://creativecommons.org/licenses/by-nc-nd/4.0/.

© The Author(s) 2024